Heterobimetallic Oxygenation

DOI: 10.1002/anie.201001914

Monooxygenase-Like Reactivity of an Unprecedented Heterobimetallic {FeO_2Ni} Moiety**

Shenglai Yao, Christian Herwig, Yun Xiong, Anna Company, Eckhard Bill, Christian Limberg, and Matthias Driess**

In memory of Herbert Schumann

The soluble methane monooxygenase, sMMO, catalyzes the remarkable oxidation of methane to methanol under ambient conditions,[1] as well as the oxygenation of a large variety of other substrates, such as ethers and alkanes and also aromatic, heterocyclic, and chlorinated compounds.[2] The activation of dioxygen occurs at a diiron moiety within the hydroxylase subunit, for which currently a three-stage model is postulated: 1) the initial interaction of dioxygen with the diiron(II) center leading to $MMOH_{peroxo}$,[3–5] 2) O–O bond cleavage under formation of $MMOH_Q$, which contains a high-valent dioxo-diiron(IV) unit,[3,6,7] and finally 3) the monooxygenation of the substrate by $MMOH_Q$, either in a concerted manner or by a hydrogen-abstraction/oxygen-rebound mechanism (Scheme 1).[5,8] Two-electron reduction of the resulting $MMOH_{ox}$ by NADH then reinitiates the catalytic cycle.[9] Actual knowledge concerning the sMMO has initiated a large amount of model chemistry,[10] and today several synthetic compounds containing high-valent Fe^{IV}–O–Fe^{IV} units are known,[11–13] among them even an example with the {$Fe^{IV}_2(\mu_2\text{-}O)_2$} diamond core structure[13] postulated for intermediate $MMOH_Q$. However, the secret of the much higher reactivity of $MMOH_Q$ in comparison to the model compounds has yet to be unraveled,[10] which calls for further refinements and even more general studies.

This background inspired us to follow not a biomimetic but bio-modifying approach to gain insight into the oxygenase activity of merely one iron center in a synthetic, heterobimetallic {FeO_2M'} core toward organic substrates (M' = transition metal other than iron). Of particular interest was the identification of the electronic situation of the bridging O_2 unit, which could correspond to either a peroxo ligand or a bis(μ_2-oxo) moiety, depending on the electronic nature (such as the oxidation potential) of M'; the latter, in turn, may thus imply different oxygenase activities. To date, synthetic heterobimetallic {FeO_2M'} systems are very rare; a well-characterized representative is a peroxo-bridged heme–copper complex, which contains a Fe^{III}–O–O–Cu^{II} unit and thus models the cytochrome c oxidase.[14] However, systems of the type $Fe^{II}/O_2^{2-}/M'^{II}$ with M' having a higher oxidation potential than iron(II) (for example, nickel(II), which serves a biological function in combination with reduced O_2 species such as superoxides) are hitherto unknown. This prompted us to synthesize a {FeO_2Ni} complex by facile oxidative addition of an iron(I) precursor to a nickel(II) superoxo complex. The desired peroxo complex {$Fe^{II}(\mu_2\text{-}O_2)Ni^{II}$} formed initially could be expected to subsequently rearrange under O–O bond scission to give {$Fe^{III}(\mu_2\text{-}O)_2Ni^{III}$} or {$Fe^{IV}(\mu_2\text{-}O)_2Ni^{II}$} compounds. The latter appear interesting for structure-reactivity studies, in particular to understand the electronic situations of iron and oxygen as active sites in heterobimetallic analogues of sMMO models for C–H bond activation. A further motivation to study such cores is the fact that iron(II) and peroxide are ingredients for Fenton chemistry,[15] which under acidic conditions leads to iron(III) and OH radicals along with {$Fe^{IV}=O$} intermediates. This system catalyzes the oxidation of hydrocarbons via organic radicals, and it seemed appealing to investigate the effects of replacing H^+ by the Lewis acidic nickel(II) center. Herein we present the assembly of the first heterobimetallic {FeO_2Ni} complexes, which successively led to selective C–H activation.

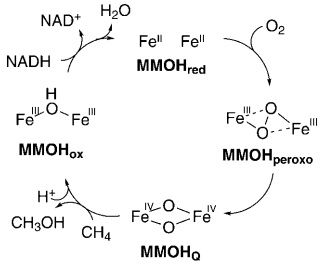

Scheme 1. Proposed mechanism for the activation of dioxygen in the hydroxylase subunit of the sMMO (MMOH).

[*] Dr. S. Yao, Dr. Y. Xiong, Dr. A. Company, Prof. Dr. M. Driess
Technische Universität Berlin
Institute of Chemistry: Metalorganics and Inorganic Materials
Sekr. C2, Strasse des 17. Juni 135, 10623 Berlin (Germany)
Fax: (+49) 30-314-29732
E-mail: matthias.driess@tu-berlin.de
Homepage: http://www.driess.tu-berlin.de
Dr. E. Bill
Max-Planck-Institut für Bioanorganische Chemie
Stiftsstrasse 34-36, 45470 Mülheim/Ruhr (Germany)
Dr. C. Herwig, Prof. Dr. C. Limberg
Humboldt-Universität zu Berlin, Institut für Chemie
Brook-Taylor-Strasse 2, 12489 Berlin (Germany)
E-mail: christian.limberg@chemie.hu-berlin.de
Homepage: http://www.chemie.hu-berlin.de/aglimberg/

[**] Financial support from the Cluster of Excellence "Unifying Concepts in Catalysis" (EXC 314/1) (administered by the TU Berlin and funded by the Deutsche Forschungsgemeinschaft) is gratefully acknowledged. A.C. thanks the European Commission for a Marie-Curie Fellowship.

Supporting information for this article is available on the WWW under http://dx.doi.org/10.1002/anie.201001914.

Treatment of a green solution of superoxo complex $[L^{Me}Ni^{II}O_2]$ (**1**; $L^{Me} = [HC(CMeNC_6H_3(iPr)_2)_2])$[16] in toluene with the convenient iron(I) precursor $[L^{Me}FeN_2FeL^{Me}]$[17] in a molar ratio of 2:1 at −60 °C led to a brown solution, from which dark brown crystals of the paramagnetic complex **2a** could be obtained in 79% yield (Scheme 2). The composition of **2a** was confirmed by EI mass spectrometry and elemental analysis (see Supporting Information). Its molecular structure, however, could only be determined unequivocally by single-crystal X-ray diffraction analysis (Figure 1); suitable single crystals of **2a** were obtained from hexane solutions by cooling.[31]

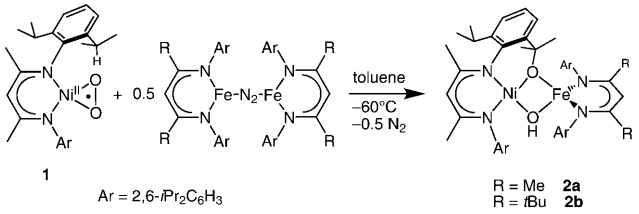

Scheme 2. Synthesis of **2a** and **2b** starting from **1** and iron(I) precursors.

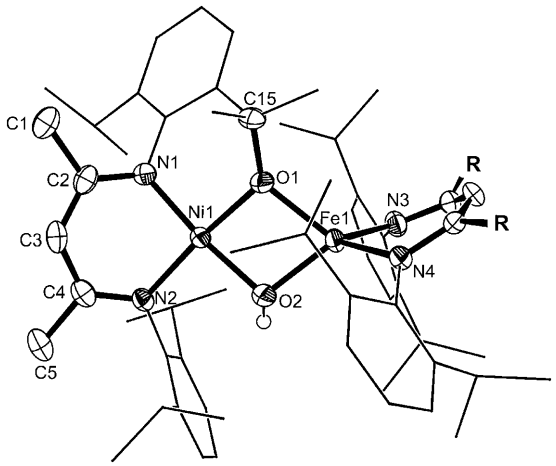

Figure 1. Molecular structure of **2a** (R = Me) and **2b** (R = *t*Bu) in the crystal. Ellipsoids set at 50% probability; hydrogen atoms except the one on O2 omitted for clarity. Selected bond lengths [Å] and angles [°]: **2a**: Ni1–N1 1.866(2), Ni1–N2 1.894(2), Ni1–O1 1.866(2), Ni1–O2 1.888(2), Fe1–O2 1.951(2), Fe1–O1 2.013(2), Fe1–N3 2.017(3), Fe1–N4 2.017(3), O1–C15 1.438(3), Ni1···Fe1 2.9603(6), O1···O2 2.455(2); O1-Ni1-O2 81.66(9), N1-Ni1-N2 94.2(1), O2-Fe1-O1 76.52(9), N3-Fe1-N4 95.1(1), Ni1-O1-Fe1 99.42(9), Ni1-O2-Fe1 100.9(1). **2b**: Ni1–N1 1.864(3), Ni1–N2 1.894(3), Ni1–O1 1.870(2), Ni1–O2 1.884(3), Fe1–O2 1.963(3), Fe1–O1 2.034(2), Fe1–N3 1.999(3), Fe1–N4 2.056(2), O1–C15 1.444(4), O1···O2 2.456(3), Ni1···Fe1 2.996(3); O1-Ni1-O2 81.7(1), N1-Ni1-N2 93.9(1), O2-Fe1-O1 75.82(9), N3-Fe1-N4 95.6(1), Ni1-O1-Fe1 100.14(9), Ni1-O2-Fe1 102.3(1).

The analysis revealed that **2a** crystallizes as a hexane solvate in the triclinic space group $P\bar{1}$. It contains β-diketiminato-ligated nickel(II) and iron(II) centers in square planar and tetrahedral coordination environments, respectively. Unexpectedly, the metal atoms are bridged by a μ-hydroxide ligand and a μ-alkoxide unit derived from C–H activation of a *i*Pr group belonging to the β-diketiminato ligand bound at the nickel site. The latter tridentate ligand and the β-diketiminato iron unit are orthogonal to each other and slightly puckered.

The Ni–N distances in **2a** (1.866(2) and 1.894(2) Å) are shorter than those in $[L^{Me}Ni^{II}(\mu_2\text{-}OH)_2Ni^{II}L^{Me}]$ (1.920(4) and 193.1(4) Å),[16] whilst the Ni–O distances are very similar in both complexes (1.866(2) and 1.888(2) Å in **2a**, compared to 1.861(7) and 1.865(7) Å found for the square-planar-coordinated nickel center within $[L^{Me}Ni^{II}(\mu_2\text{-}OH)_2Ni^{II}L^{Me}]$[16]). The Fe–N distances in **2a** (both 2.017(3) Å) are similar to those observed in other β-diketiminato iron(II) complexes with a four-coordinate iron center.[18a] The Fe1–O2 distance (1.951(2) Å) is shorter than corresponding distances observed in a comparable β-diketiminato-ligated bis(μ-hydroxo) diiron(II) complex (2.059(6) and 2.082(3) Å),[18b] but not as short as those found in a β-diiminato complex containing a Fe^{III}–O–Fe^{III} unit (1.769(2) Å),[19] which prior to any further analysis already argues against a Ni^{II}–O–Fe^{III} unit in **2a**, and in fact the presence of a hydrogen atom at the O2 atom has been shown by crystallography and IR spectroscopy ($\tilde{\nu}_{OH} = 3640\ cm^{-1}$). The C15–O1 distance (1.438 (3) Å) falls within the common C–O single bond range, whereas the O···O distance of 2.455(2) Å and the Ni···Fe distance of 2.9603(6) Å imply that there are no attractive interactions (bonds) between the respective atoms.

To probe whether selectively the L^{Me}Ni and not the L^{Me}Fe moiety experiences C–H activation with subsequent formation of bridging μ-OH and μ-alkoxo ligands, we employed $[LtBuFeN_2FeLtBu]$[17b] as a distinguishable derivative of the iron(I) precursor $[L^{Me}FeN_2FeL^{Me}]$. In a similar procedure as described above for the synthesis of **2a**, paramagnetic **2b** could be obtained as dark brown crystals in 74% yield (Scheme 2). It has been fully characterized by HR-ESI mass spectrometry, C,H,N elemental analysis, and IR spectroscopy. An X-ray diffraction analysis of **2b**[31] revealed almost identical geometric parameters for the NiO_2Fe core compared to those in **2a** (Figure 1), except for a slightly longer Ni···Fe distance (2.996 Å in **2b** versus 2.960 Å in **2a**). The *t*Bu residues are found at the intact diketiminato moiety, thus proving that C–H bond cleavage occurs selectively at an *i*Pr group of the diketiminato ligand bound to nickel. Both **2a** and **2b** are paramagnetic in the solid state and also in solution (^{1}H NMR). Magnetic measurements performed for solutions (Evans method[20] using C_6D_6 as solvent) of **2a** and **2b** revealed μ_{eff} values of 4.83 and 4.85 μ_B at room temperature, respectively, corresponding to a spin-only value of four unpaired electrons. Because it seemed unlikely that the unpaired electrons belong to the β-diketiminatonickel moiety, the spin-only value suggested the presence of high-spin iron(II), as confirmed by Mössbauer measurements on solid **2a** through a signal with a characteristic, relatively large isomeric shift value of 0.9 $mm\,s^{-1}$ (Figure 2). The value is typical of a four-coordinate center and resembles the shifts observed for iron(II) halides ($FeCl_2$, $\delta = 1.1\ mm\,s^{-1}$)[21] or the quasi-tetrahedral $\{Fe^{II}S_4\}$ sites in iron–sulfur clusters (rubredoxin $\delta = 0.7\ mm\,s^{-1}$).[22] The large quadrupole splitting ($\Delta E_Q = 2.51\ mm\,s^{-1}$) indicates a large valence contribution

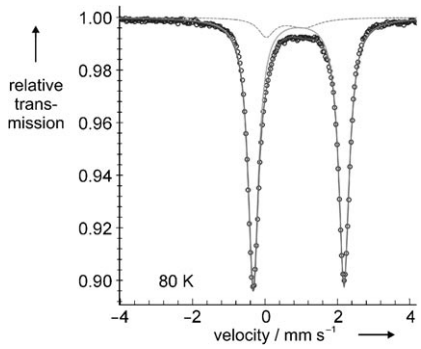

Figure 2. Zero-field Mössbauer spectrum of solid **2a** recorded at 80 K. The lines represent a fit with Lorentzian doublets ($\delta = 0.93$ mm s^{-1}, $\Delta E_Q = 2.51$ mm s^{-1}); the dotted trace is a 9% contribution with parameters $\delta = 0.54$ mm s^{-1}, $\Delta E_Q = 1.04$ mm s^{-1}, indicating a minor ferric high-spin contamination.

to the electric field gradient, as expected for the $3d^6$ configuration in distorted tetrahedral symmetry with a low lying x^2-y^2 or z^2 orbital.

Accordingly, SQUID measurements of **2a** show the presence of $S = 2$ for the $\{Fe^{II}Ni^{II}\}$ unit (Figure 3). A spin-Hamiltonian simulation reveals moderately strong zero-field splitting ($|D| = 6.9$ cm^{-1}, $g = 2.02$), similar to what was found for other tetrahedrally coordinated high-spin iron(II) centers.[23]

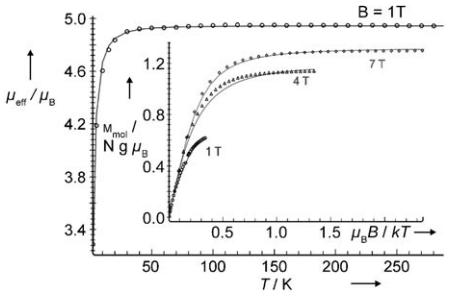

Figure 3. Temperature dependence of the effective magnetic moment of **2a** and temperature dependence of the molar magnetization at $B = 1$, 4, and 7 T sampled on a $1/T$ inverse temperature scale (inset). The solid lines are the result of a global spin-Hamiltonian simulation for $S = 2$ with parameters $g_{av} = 2.02$, $D = -6.9(6)$ cm^{-1}, $E/D = 0.0(2)$.

Having identified the final product of the reaction between **1** and $L^{Me}FeN_2FeL^{Me}$ as **2a**, we attempted to observe an intermediate of this conversion. In fact, monitoring the reaction at −70 °C by UV/Vis spectroscopy revealed the formation of a short-lived species with two bands at 560 and 650 nm, which, however, could not be identified because it decays within seconds (see Supporting Information). To bridge this knowledge gap concerning the initial product that is responsible for the strikingly selective C–H activation, we performed DFT calculations (B3LYP/6-31G*).[24] First we carried out a geometry optimization for a simplified model of **2a** (see Supporting Information). Singlet, triplet, quintet, and septet spin states were considered, and the quintet state turned out to be the most stable (45.7 kJ mol^{-1} lower in energy as compared to the triplet state); testing for broken-symmetry states did not lead to further stabilization. Thus, a final geometry optimization was carried out for the complete molecule **2a** in the quintet state, and the results were evaluated. The four unpaired spins were found to be located exclusively at the iron center, whereas the nickel ion has a closed-shell configuration, which is in excellent agreement with data obtained by Mössbauer and magnetic measurements. The calculated structure also agrees very well with the experimental metric data, and altogether this validates the theoretical method chosen. Subsequently, the initial product **I** of the reaction of **1** with $[L^{Me}FeN_2FeL^{Me}]$ that further reacts in a second step to give **2a** was addressed (see Scheme 3). On

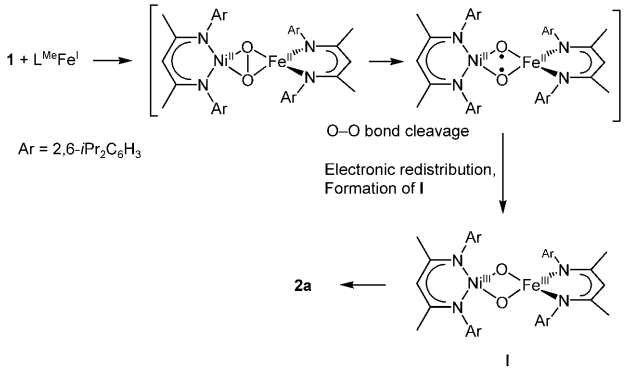

Scheme 3. Formation of transient spieces **I** and its conversion into **2a**.

the basis of our previous results showing that reduction of **1** with elemental potassium leads to a nickel(II) peroxide species that exhibits no tendency towards C–H activation,[25] we can exclude that $[L^{Me}FeN_2FeL^{Me}]$ acts merely as a reducing agent of **1** to give an ordinary nickel(II) peroxide analogue triggering C–H activation.

Further calculations were therefore carried out for the elucidation of the actual electronic structure of an intermediate **I** corresponding to the formula $[L^{Me}FeO_2NiL^{Me}]$. To determine its favorable spin state again (as for **2a**), geometry optimizations were first carried out for a simplified model (in which methyl and isopropyl residues of the L^{Me} ligand were omitted) in singlet, triplet, quintet, and septet spin states. This procedure was performed without imposing any restrictions on the system, and strikingly, a local minimum with an intact O–O bond never emerged for any of the spin states investigated; that is, a $\{Fe(\mu_2\text{-}O)_2Ni\}$ core is generated. Akin to **2a**, the quintet state turned out to be the most stable, and broken symmetry states were not found to be of relevance, so that, notably, the C–H activation process proceeds entirely on the quintet potential energy surface. For the further analysis of the electronic structure the complete molecule **I** (including all residues) in the quintet state was subjected to a geometry optimization, and the result is shown in Figure 4.

Remarkably, both metal centers exhibit a distorted square planar coordination geometry, probably as the isopropyl groups can pack quite efficiently this way. The unpaired spin density is distributed such that the nickel center has 0.8 spins

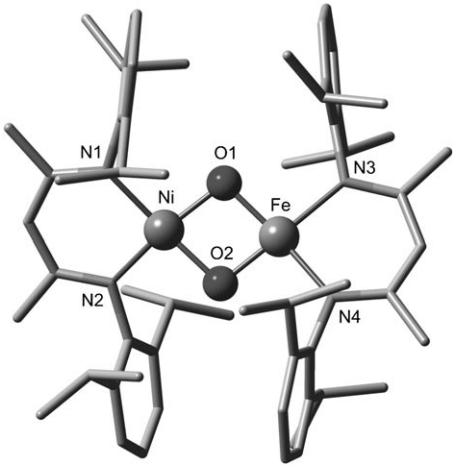

Figure 4. Optimized molecular structure for the quintet state of **I**. Hydrogen atoms are omitted for clarity. Selected bond lengths [Å]: Ni–N1 1.944, Ni–N2 1.905, Ni–O1 1.7857, Ni–O2 1.827, Fe–O2 1.764, Fe–O1 1.808, Fe–N3 2.024, Fe–N4 2.019, Ni···Fe 2.720, O1···O2 2.345.

(indicating nickel(III)) and 2.9 spins are on iron (suggesting iron(III) in an intermediate spin state of 3/2), whilst the oxygen atoms carry an averaged unpaired spin density of only 0.08. Insofar, the electronic situation in **I** is entirely different compared to one calculated for an analogous $\{NiO_2Zn\}$ scenario:[25] As zinc(II) is redox-inert, the oxygen atoms mainly preserve their radical character (spin density of 0.56). The latter is only diluted somewhat by withdrawing electron density from nickel(II), which therefore carries 40% of the unpaired spin density. Accordingly, a corresponding complex generated in-situ from a nickel(II) peroxide and zinc(II) reacts further by net abstraction of two hydrogen atoms from the surroundings to give the corresponding $\{Ni^{II}(\mu\text{-}OH)_2Zn\}$ compound.[25] In contrast, **I** contains a subunit that may be regarded best as $\{Fe^{III}(\mu_2\text{-}O)_2Ni^{III}\}$, as shown in Scheme 3 (in line with the calculated spin-density distribution). Consequently, the results of the calculations clearly show that in **I** unpaired spin density is shifted almost entirely from the bridging oxo ligands to the iron and the nickel centers. Thus, while the aforementioned $\{Ni^{II}(\mu\text{-}O)_2Zn\}$ unit behaves like an oxygen-centered diradical, **I** is less reactive but more selective and oxygenates one of the *i*Pr residues belonging to the ligands, most likely by a hydrogen-abstraction/oxygen-rebound mechanism followed by a proton shift. Comparison of the energies of **2a** and **I** reveals a driving force for the latter process of 176 kJ mol^{-1}. In principle, this kind of reactivity is reminiscent of the one proposed for the sMMO, but it has to be borne in mind that the intermediate **I** has two oxidation equivalents less available than the intermediate Q of the sMMO (see above). Strikingly, **I** is still capable of realizing a monooxygenation, as the reduction of the iron center in course of hydrocarbon oxidation produces back iron(II), whereas $MMOH_Q$ rests after formation of the thermodynamically stable $\{Fe^{III}\text{–}O(H)\text{–}Fe^{III}$ unit$\}$. Therefore, although $MMOH_Q$ incorporates all four oxidation equivalents originating from activated O_2, it utilizes only two of those for hydrocarbon oxygenation. Consistently, it has been found that $\{Fe^{III}(\mu\text{-}O)_2Fe^{IV}\}$ model compounds are only capable of performing one-electron oxidation processes.[26–29] By contrast **I** can apply both of its oxidation equivalents for oxygenation, as the thermodynamic sink of a $\{Fe^{III}\text{–}O\text{–}Fe^{III}\}$ subunit is avoided by replacement of one of the iron centers by nickel.

However, why oxygenation occurs selectively on one of the C–H groups of the β-diketiminato ligand coordinated at nickel cannot be rationalized in light of the results of our calculations. There are neither complex-induced proximity effects apparent nor do the positions of the relevant orbitals of oxygen indicate any favorable interactions. On the contrary, within **I** the methine hydrogen atoms of the *i*Pr groups belonging to the ^{Me}LFe unit are located more closely to the oxo ligands.[30] This calls for further synthesis and experimental investigations of related heterobimetallic MO_2Ni systems (e.g., M = Cr, Mn, Co), which could help to understand oxygenase activity and selectivity. Corresponding studies are currently in progress.

Received: March 31, 2010
Revised: June 9, 2010
Published online: August 18, 2010

Keywords: bioinorganic chemistry · dioxgen activation · iron · nickel · oxygenases

[1] a) D. W. Ribbons, *J. Bacteriol.* **1975**, *122*, 1351–1363; b) G. M. Tonge, D. E. F. Harrison, C. J. Knowles, I. J. Higgins, *FEBS Lett.* **1975**, *58*, 293–299; c) H. Dalton, *Adv. Appl. Microbiol.* **1980**, *26*, 71–87.

[2] a) K. K. Andersson, W. A. Froland, S.-K. Lee, J. D. Lipscomb, *New J. Chem.* **1991**, *15*, 411–415; b) T. Bosma, D. B. Janssen, *Appl. Microbiol. Biotechnol.* **1998**, *50*, 105–112; Y. Jin, J. D. Lipscomb, *J. Biol. Inorg. Chem.* **2001**, *6*, 717–725; c) J. Green, H. Dalton, *J. Biol. Chem.* **1989**, *264*, 17698–17703; B. G. Fox, J. G. Bornemann, L. P. Wackett, J. D. Lipscomb, *Biochemistry* **1990**, *29*, 6419–6427; d) M. J. Rataj, J. E. Kauth, M. I. Donnelly, *J. Biol. Chem.* **1991**, *266*, 18684–18690; e) S. J. Lippard, *J. Am. Chem. Soc.* **2005**, *127*, 7370–7378.

[3] K. E. Liu, A. M. Valentine, D. Wang, B. H. Huynh, D. E. Edmondson, A. Salifoglou, S. J. Lippard, *J. Am. Chem. Soc.* **1995**, *117*, 10174–10185.

[4] K. E. Liu, A. M. Valentine, D. Qui, D. E. Edmondson, E. H. Appelman, T. G. Spiro, S. J. Lippard, *J. Am. Chem. Soc.* **1995**, *117*, 4997–4998.

[5] A. M. Valentine, S. S. Stahl, S. J. Lippard, *J. Am. Chem. Soc.* **1999**, *121*, 3876–3887.

[6] S.-K. Lee, B. G. Fox, W. A. Froland, J. D. Lipscomb, E. Münck, *J. Am. Chem. Soc.* **1993**, *115*, 6450–6451.

[7] L. Shu, J. C. Nesheim, K. Kauffmann, E. Münck, J. D. Lipscomb, L. Que, Jr., *Science* **1997**, *275*, 515–518.

[8] K. E. Liu, D. Wang, B. H. Huynh, D. E. Edmondson, A. Salifoglou, S. J. Lippard, *J. Am. Chem. Soc.* **1994**, *116*, 7465–7466.

[9] a) B. J. Wallar, J D. Lipscomb, *Chem. Rev.* **1996**, *96*, 2625–2657; b) M. Merkx, D. A. Kopp, M. H. Sazinsky, J. L. Blazyk, J. Müller, S. Lippard, *Angew. Chem.* **2001**, *113*, 2860–2888; *Angew. Chem. Int. Ed.* **2001**, *40*, 2782–2807.

[10] I. Siewert, C. Limberg, *Chem. Eur. J.* **2009**, *15*, 10316–10328.

[11] A. Ghosh, F. T. de Oliveria, T. Yano, T. Nishioka, E. S. Beach, I. Kinoshita, E. Münck, A. D. Ryabov, C. P. Horwitz, T. J. Collins, *J. Am. Chem. Soc.* **2005**, *127*, 2505–2513.

[12] G. Xue, A. T. Fiedler, M. Martinho, E. Münck, L. Que, Jr., *Proc. Natl. Acad. Sci. USA* **2008**, *105*, 20615–20620.

[13] G. Xue, D. Wang, R. De Hont, A. T. Fiedler, X. Shan, E. Münck, L. Que, Jr., *Proc. Natl. Acad. Sci. USA* **2007**, *104*, 20713 – 20718.
[14] T. Chishiro, Y. Shimazaki, F. Tani, Y. Tachi, Y. Naruta, S. Karasawa, S. Hayami, Y. Maeda, *Angew. Chem.* **2003**, *115*, 2894 – 2897; *Angew. Chem. Int. Ed.* **2003**, *42*, 2788 – 2791.
[15] S. Goldstein, D. Meyerstein, *Acc. Chem. Res.* **1999**, *32*, 547 – 550; see also: J. Bautz, M. R. Bukowski, M. Kerscher, A. Stubna, P. Comba, A. Lienke, E. Münck, L. Que, Jr., *Angew. Chem.* **2006**, *118*, 5810 – 5813; *Angew. Chem. Int. Ed.* **2006**, *45*, 5681 – 5684; F. Li, J. England, L. Que, Jr., *J. Am. Chem. Soc.* **2010**, *132*, 2134 – 2135.
[16] S. Yao, E. Bill, C. Milsmann, K. Wieghardt, M. Driess, *Angew. Chem.* **2008**, *120*, 7218 – 7221; *Angew. Chem. Int. Ed.* **2008**, *47*, 7110 – 7113.
[17] a) J. M. Smith, A. R. Sadique, T. R. Cundari, K. R. Rodgers, G. Lukat-Rodgers, R. J. Lachicotte, C. J. Flaschenriem, J. Vela, P. L. Holland, *J. Am. Chem. Soc.* **2006**, *128*, 756 – 769; b) J. M. Smith, R. J. Lachicotte, K. A. Pittard, T. R. Cundari, G. Lukat-Rodgers, K. R. Rodgers, P. L. Holland, *J. Am. Chem. Soc.* **2001**, *123*, 9222 – 9223.
[18] a) See for example: N. A. Eckert, J. M. Smith, R. J. Lachicotte, P. L. Holland, *Inorg. Chem.* **2004**, *43*, 3306 – 3321; b) Y. Yu, A. R. Sadique, J. M. Smith, T. R. Dugan, R. E. Cowley, W. W. Brennessel, C. J. Flaschenriem, E. Bill, T. R. Cundari, P. L. Holland, *J. Am. Chem. Soc.* **2008**, *130*, 6624 – 6638.
[19] M. F. Pilz, C. Limberg, S. Demeshko, F. Meyer, B. Ziemer, *Dalton Trans.* **2008**, 1917 – 1923.
[20] a) D. F. Evans, *J. Chem. Soc.* **1959**, 2003 – 2005; b) T. Ayers, R. Turk, C. Lane, J. Goins, D. Jameson, S. J. Slattery, *Inorg. Chim. Acta* **2004**, *357*, 202 – 206.
[21] N. N. Greenwood, T. C. Gibb, *Mössbauer Spectroscopy*, Chapman and Hall Ltd., London, **1971**.
[22] a) C. E. Schulz, P. G. Debrunner, *J. Phys. (Paris)* **1976**, *37*, C6 – C153; b) V. Schünemann, H. Winkler, *Rep. Prog. Phys.* **2000**, *63*, 263 – 353.
[23] A. X. Trautwein, E. Bill, E. L. Bominaar, H. Winkler, *Struct. Bonding (Berlin)* **1991**, *78*, 1 – 95.
[24] Software for DFT calculations: a) M. J. Frisch et al., Gaussian03 Rev. D.01, Gaussian, Inc., Wallingford CT, **2004**; b) F. Neese, ORCA, Version 2.7, University of Bonn, **2009**; see Supporting Information.
[25] S. Yao, Y. Xiong, M. Vogt, H. Grützmacher, C. Herwig, C. Limberg, M. Driess, *Angew. Chem.* **2009**, *121*, 8251 – 8254; *Angew. Chem. Int. Ed.* **2009**, *48*, 8107 – 8110.
[26] C. Kim, Y. Dong, L. Que, Jr., *J. Am. Chem. Soc.* **1997**, *119*, 3635 – 3636.
[27] Moreover, the few known mononuclear $Fe^{IV}=O$ compounds also mainly perform single-electron oxidations to yield iron(III) complexes owing to very slow rebound rates[28] or comproportionation.[29]
[28] C. V. Sastri, J. Lee, K. Oh, Y. Jin Lee, J. Lee, T. A. Jackson, K. Ray, H. Hirao, W. Shin, J. A. Halfen, J. Kim, L. Que, Jr., S. Shaik, W. Nam, *Proc. Natl. Acad. Sci. USA* **2007**, *104*, 19181 – 19186.
[29] A. Mukherjee, M. Martinho, E. L. Bominaar, E. Münck, L. Que, Jr., *Angew. Chem.* **2009**, *121*, 1812 – 1815; *Angew. Chem. Int. Ed.* **2009**, *48*, 1780 – 1783.
[30] Still, for a simplified model it could be shown that the product of C–H activation at the ^{Me}LNi unit is favored by 24.4 kJ mol^{-1} in comparison to that that results from attack at the ^{Me}LFe unit (see Supporting Information).
[31] See the Supporting Inofrmation for details of the crystal structure determination. CCDC 770721 (**2a**) and CCDC 770722 (**2b**) contain the supplementary crystallographic data for this paper. These data can be obtained free of charge from The Cambridge Crystallographic Data Centre via www.ccdc.cam.ac.uk/data_request/cif.

